

Moreover, Wherry *et al.* showed that not only the persistence of a viral Ag, but also the initial Ag level is an important factor determining the quality of the antiviral memory response.¹³

Hepatitis C virus core protein has been reported to suppress T-cell response. HCV core-mediated inhibition of T-cell response can occur via either modulation of pro-inflammatory cytokine production by antigen-presenting cells (APC; i.e. monocyte and dendritic cells)¹⁴ or direct effect on T cells.^{15–17} Because the liver is the major site of HCV infection, it is crucial to understand the regulation of host immunity by HCV core in the liver compartment and the impact of HCV core-induced immune dysregulation in facilitating HCV persistence.

Hepatitis C virus does not infect small laboratory animals. The lack of a small animal model has hampered studies attempting to elucidate the mechanism of HCV-mediated suppression of antiviral CD8 T-cell activity and caused difficulty in the development of a therapeutic and/or prophylactic HCV vaccine.

Adenoviral vectors efficiently and reproducibly transfer foreign DNA into the livers of immunocompetent experimental animals. *i.v.* administration of adenoviral vectors of more than 10^9 infectious units/mouse results in infection and Ag expression in more than 90% of hepatocytes and acute self-limiting viral hepatitis.^{18,19}

In this study, to develop a useful animal model in the development of immunotherapy for chronic hepatitis C, we examined the responses of intrahepatic CD8 T cells of HCV core transgenic (Tg) mice with various infectious doses of HCV-NS3-recombinant adenovirus (Ad-HCV-NS3).

METHODS

Mice

C57BL/6 MICE WERE purchased from Clea Japan (Tokyo, Japan), and Tokyo Laboratory Animal Science (Tokyo, Japan). Production of HCV core Tg mice has been described.²⁰ The core gene of HCV placed downstream of a transcriptional regulatory region from hepatitis B virus, which has been shown to allow an expression of genes in Tg mice without interfering with mouse development,²¹ was introduced into C57BL/6 mouse embryos (Clea Japan). Eight- to 10-week-old mice were used for all experiments. The mice were housed in appropriate animal care facilities at Saitama Medical University (Saitama, Japan) and were handled according to international guidelines. The experimental

protocols were approved by the Animal Research Committee of Saitama Medical University (#855).

HCV-NS3 recombinant adenovirus

Adenovirus HCV-NS3 expressing the fusion protein, comprising the entire HCV-NS3 and 3X flag, was constructed by using the AdEasy XL adenoviral vector system (Agilent Technologies, Santa Clara, CA, USA). The HCV-NS3 gene corresponding to amino acid residues 1027–1657 was amplified from the plasmid pBRTM/HCV1-3011con which contains the entire DNA sequence derived from the HCV H77 clone (kindly provided by Charls M. Rice, The Rockefeller University, New York, NY, USA)²² by polymerase chain reaction. The recombinant Ad-HCV-NS3 vector was linearized by *PacI* digestion, and then transfected into 293 cells using Lipofectamine LTX (Invitrogen, Carlsbad, CA, USA) to generate adenovirus. Ad-HCV-NS3 expressing transgene NS3 was amplified in 293 cells, purified by a series of cesium chloride ultracentrifugation gradients and stored at -80°C until use. Mice were injected *i.v.* with 2×10^7 , 1×10^9 and 1×10^{10} plaque-forming units (PFU) of Ad-HCV-NS3 or Ad ψ 5 control vector. The experimental protocol regarding construction of recombinant adenovirus and infection of mice was approved by the Recombinant DNA Advisory Committee of Saitama Medical University (#1073).

Isolation of intrahepatic leukocytes

The liver was perfused with phosphate-buffered saline (PBS) plus 0.05% collagenase via the portal vein. Perfused livers were smashed through a 100- μm cell strainer (BD Biosciences, San Jose, CA, USA). The cell suspension was centrifuged with 35% Percoll at 320 g for 10 min, and the cell pellet was cultured in a plastic Petri dish in RPMI-1640 medium supplemented with 10% fetal calf serum (FCS; R-10) for 1.5 h to remove adherent cells. Then, non-adherent cells were harvested, washed twice with R-10 and used as intrahepatic lymphocytes (IHL). Adherent cells were used as intrahepatic APC).

Intracellular IFN- γ staining

The IHL were resuspended in R-10. In each well of a 96-well round-bottomed plate, 2×10^6 IHL were incubated for 5 h at 37°C in R-10 containing 50 ng/mL phorbol myristate acetate (PMA; Sigma-Aldrich, St Louis, MI, USA), 1 μM ionophore A23187 (Sigma-Aldrich) and 1 $\mu\text{g}/\text{mL}$ brefeldin-A (BD Biosciences). The cells were then washed twice with ice-cold PBS (–) and incubated for 10 min at 4°C with a rat antimouse

CD16/CD32 monoclonal Ab (mAb; Fc Block; BD Biosciences) at a concentration of 1 µg/well. Following incubation, the cells were washed twice with ice-cold PBS (–) and stained with a PE-conjugated HCV-NS3 H-2Db tetramer (Tet-603; GAVQNEVTL; Medical and Biological Laboratories, Nagoya, Japan)²³ and peridinin chlorophyll protein (PerCP)-conjugated rat antimouse CD8 MAb (clone 53-6.7; BD Biosciences) for 30 min at 4°C in staining buffer (PBS with 1% FCS and 0.1% NaN₃). After the cells were washed twice, they were fixed and permeabilized by using a Cytotfix/Cytoperm kit (BD Biosciences) and stained with a fluorescein isothiocyanate (FITC)-conjugated rat antimouse IFN-γ mAb (clone XMG1.2; BD Biosciences). After the cells were washed, flow cytometric analyses were performed with a FACScanto II flow cytometer (Becton Dickinson, Franklin Lakes, NJ, USA), and the data were analyzed with FACSDiva software (Becton Dickinson).

PD-1 and Tim-3 staining

Intrahepatic lymphocytes were prepared and treated with an antimouse CD16/CD32 mAb as described above for intracellular IFN-γ staining and then stained with a PE-conjugated HCV-NS3 H-2Db tetramer, PerCP-conjugated anti-CD8a (BD Biosciences), FITC-conjugated anti-PD-1 (eBioscience, San Diego, CA, USA) and Alexa647-conjugated anti-Tim-3 (Biolegend, San Diego, CA, USA) for 30 min at 4°C. After the cells were washed twice, they were fixed with PBS containing 1% formaldehyde and 2% FCS and analyzed by flow cytometry.

PD-L1 staining

Intrahepatic APC were prepared and treated with an antimouse CD16/CD32 mAb as described above for intracellular IFN-γ staining and then stained with a FITC-conjugated anti-CD11c (BD Biosciences) and PE-conjugated anti-PD-L1 (eBioscience) for 30 min at 4°C. After the cells were washed twice, they were fixed with PBS containing 1% formaldehyde and 2% FCS and analyzed by flow cytometry.

HCV core Ag detection

For the detection of HCV core Ag in the liver, liver tissue samples isolated 7 and 14 days post-infection were homogenized in RIPA B buffer (50 mM Tris pH 7.5, 1% NP40, 0.15 M NaCl, 1 mM phenylmethylsulfonyl fluoride) to make 10% (w/v) extract. Liver tissue extracts were assessed using Lumispot Eiken HCV Ag assay kit (Lumispot-Ag; Eiken Chemical, Tokyo, Japan).

Histology and immunohistology staining

Liver tissue samples isolated 7 and 14 days post-infection were used for histological studies. Paraffin sections (4-µm thick) were stained with hematoxylin-eosin safranin O. For immunohistology, 5-µm thick acetone-fixed frozen sections were incubated with rat anti-CD8 (BD Biosciences), followed by biotin-conjugated antirat immunoglobulin G and ABC staining system (Santa Cruz Biotechnology, Santa Cruz, CA, USA).

Persisting HCV-NS3 Ag detection

For the detection of persisting HCV-NS3 Ag in the liver, liver tissue samples isolated 21 days post-infection were homogenized in RIPA C buffer (50 mM Tris pH 7.5, 1% Triton X-100, 300 mM NaCl, 5 mM ethylenediaminetetraacetic acid, 0.02% NaN₃) to make 2% (w/v) extract and used for immune precipitation/western blot assay. Liver tissue extracts were incubated with protein-G sepharose beads for 30 min at 4°C to remove non-specifically bound proteins. After centrifugation, supernatants were incubated with anti-Flag-M2 antibody (Sigma-Aldrich) coupled protein-G sepharose beads for 2 h at 4°C. After centrifugation, HCV-NS3-3xFlag fusion protein bound to the beads were dissolved in sample buffer and separated on 10% sodium dodecylsulfate polyacrylamide gel electrophoresis gels (Mini PROTEAN TGX gel; Bio-Rad, Hercules, CA, USA) for immunoblot analysis using anti-Flag-M2 antibody and goat antimouse Ig horseradish peroxidase (KPL, Gaithersburg, MD, USA). Electrochemiluminescence Prime Western Blotting Detection Reagent (GE Healthcare, Little Chalfont, UK) was used for chemiluminescent detection.

Statistical analysis

Mann-Whitney *U*-tests were used to evaluate the significance of the differences. Correlations between parameters were tested for statistical significance by Pearson correlation.

RESULTS

Functional exhaustion of Ag-specific CD8 IHL with high infectious dose and the impaired Ag-specific CD8 IHL responses in core Tg mice

TO DETERMINE THE effect of the amount of virus dose, we evaluated hepatic inflammation and compared the magnitude of HCV-NS3-specific CD8

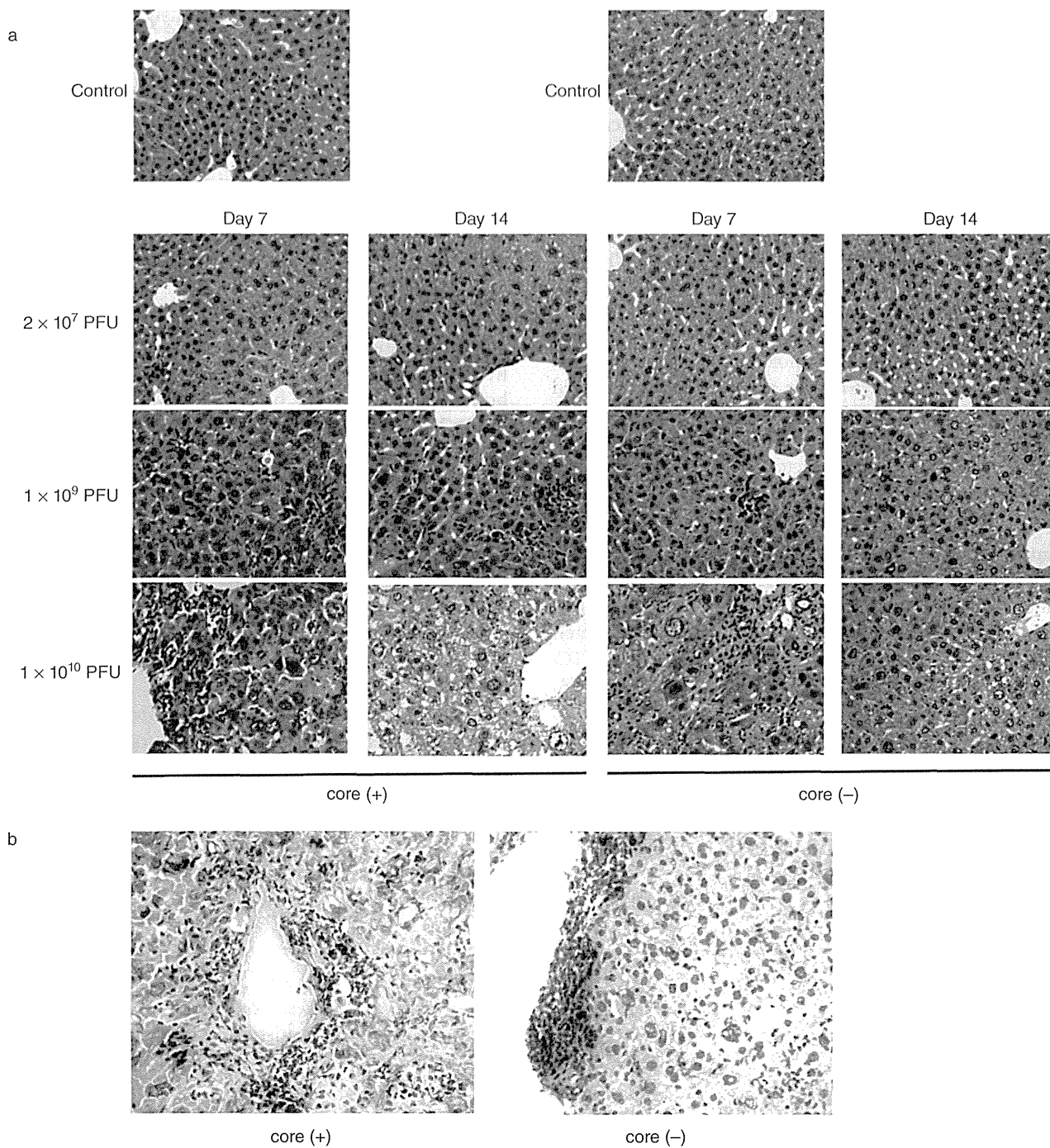


Figure 1 Adenovirus (Ad) infection-mediated hepatic inflammation in mouse liver. Hepatitis C virus (HCV) core (+) and core (-) mice were infected with 2×10^7 , 1×10^9 and 1×10^{10} plaque-forming units (PFU) of Ad-HCV-NS3 i.v. and analyzed at 7 and 14 days post-infection. (a) Harvested liver tissues were analyzed by hematoxylin–eosin staining for assessment of hepatic inflammation. (b) Frozen liver sections were analyzed by CD8 staining. Liver infected with 1×10^{10} PFU and harvested at 7 days post-infection was used (original magnifications: [a] $\times 100$; [b] $\times 200$). (c,d) The frequency and number of hepatic CD8 lymphocytes were assessed by flow cytometric analysis. There were no differences in the frequency and number of hepatic CD8 lymphocytes between core (+) mice and core (-) mice. (e) Detection of HCV core antigen in the liver. Liver tissue extracts were assessed using Lumispot Eiken HCV Ag assay kit. There were no differences in core protein expression between Ad-infected and non-infected livers. ■, day 7; □, day 14; □, day 21.

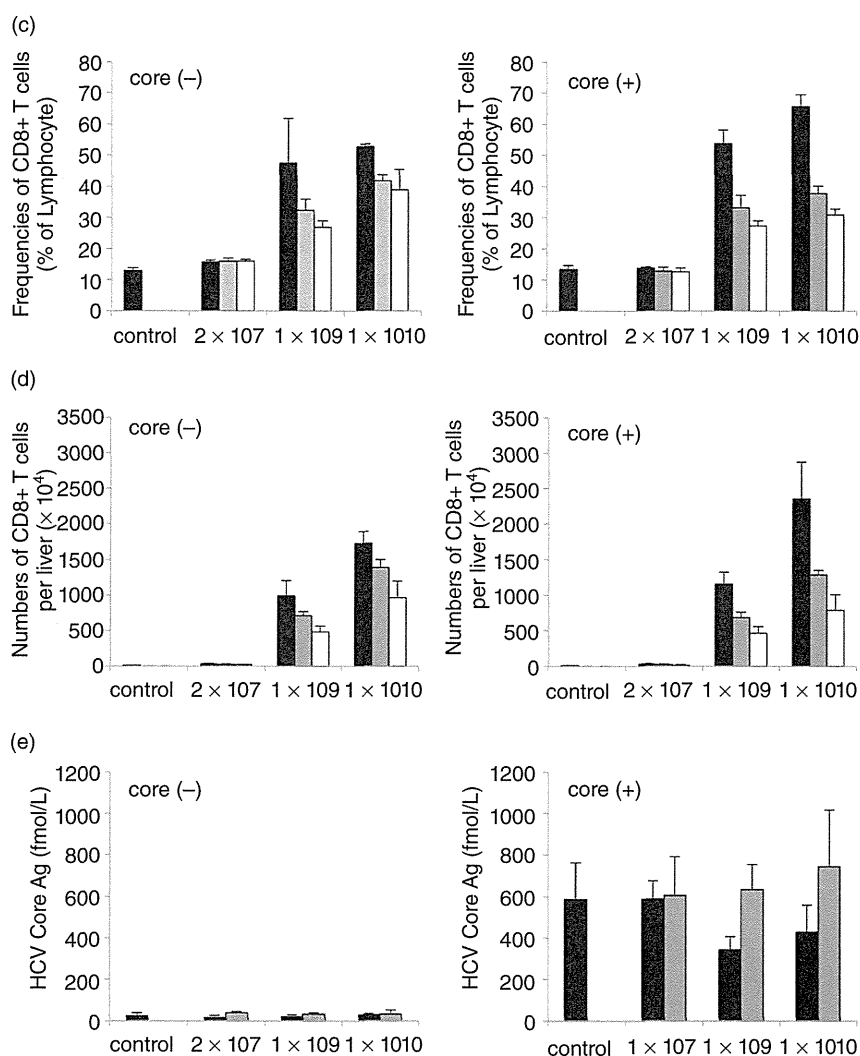


Figure 1 Continued

T-cell responses and their effector function in the liver of mice infected with 2×10^7 , 1×10^9 and 1×10^{10} PFU Ad-HCV-NS3.

In histological studies, we observed Ad-infection-mediated hepatic inflammation in mice injected with 1×10^9 and 1×10^{10} PFU. Especially, infection with 1×10^{10} PFU caused drastic infiltrations of inflammatory cells (Fig. 1a). We also observed that CD8 lymphocytes infiltrated into the lobular areas of the infected liver in mice injected with 1×10^{10} PFU (Fig. 1b). At 7 days post-infection, we found by flow cytometric assay that the numbers and the frequencies of CD8 T cells in the liver were markedly increased after infection with 1×10^9 PFU and 1×10^{10} PFU, and the increased CD8 T cells decreased with time (Fig. 1c). We did not find sig-

nificant differences between the number of CD8 T cells of core (+) and core (-) at each time point and infectious dose.

In addition, we evaluated core protein expression in the liver in each infectious dose at 7 and 14 days post-infection; there was no significant difference in core protein expression between Ad-infected and non-infected livers (Fig. 1e).

Using major histocompatibility complex (MHC) class I tetramer complexed with the H2-Db-binding HCV-NS3 GAVQNEVTL epitope, we found that i.v. infection with 2×10^7 PFU generally elicited only a weak expansion of HCV-NS3 tet⁺ CD8⁺ IHL (Fig. 2a,b) and IFN- γ HCV-NS3 tet⁺ CD8⁺ IHL (Fig. 2a,c). In contrast, infection with 1×10^9 PFU induced a significant proliferation

of HCV-NS3 tet⁺ CD8⁺ IHL (Fig. 2a,b) and IFN- γ ⁺ HCV-NS3 tet⁺ CD8⁺ IHL (Fig. 2a,c).

In each infectious dose, HCV-NS3 tet⁻ CD8⁺ IHL did not show the diminution of elicited IFN- γ production (Fig. 2a). In contrast, HCV-NS3 tet⁺ CD8⁺ IHL showed the dose-dependent diminution of elicited IFN- γ production (Fig. 2d). Especially, infection with 1×10^{10} PFU led to a dramatic diminution of the elicited IFN- γ production in HCV-NS3 tet⁺ CD8⁺ IHL (Fig. 2a,d). These indicate that high infectious dose of Ad-HCV-NS3 cause NS3 Ag-specific immunosuppression.

As shown in Figure 2(c), the number of IFN- γ -producing HCV-NS3 tetramer⁺ CD8 T cells in the liver of core (+) mice was lower than that of core (-) mice following PMA/ionophore stimulation. In addition, the percentage of IFN- γ -producing CD8 lymphocytes in tetramer⁺ CD8 IHL of core (+) mice was suppressed as compared with core (-) mice following PMA/ionophore stimulation (Fig. 2d). These suggest that the presence of HCV core gene significantly impair antiviral effector CD8 T-cell responses in the liver.

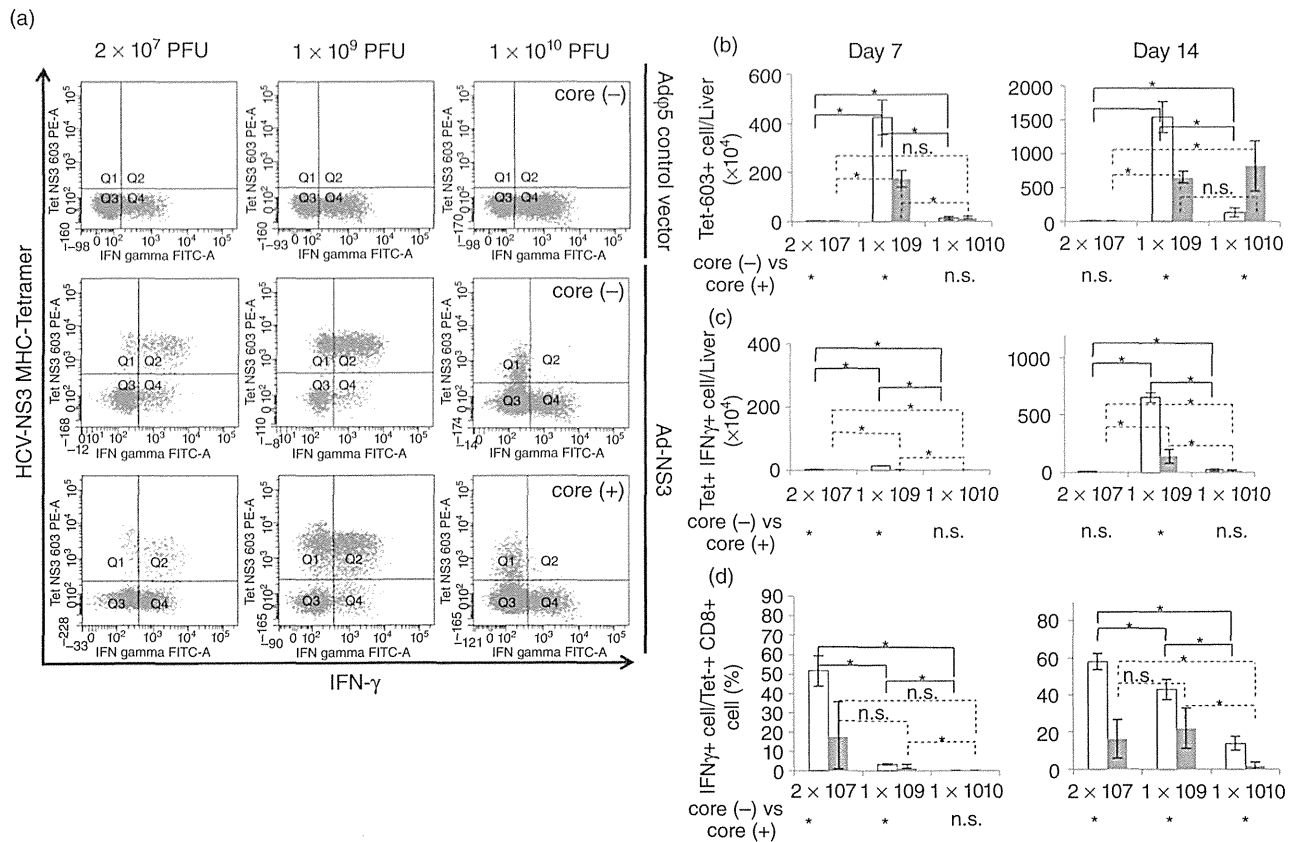


Figure 2 Impaired CD8⁺ T-cell responses in the livers of high infectious doses. (a) Flow cytometric dot gram gating on the CD8 lymphocyte at day 14 post-infection. Graded doses of adenovirus (Ad)-hepatitis C virus (HCV)-NS3 were administrated i.v and NS3-specific intrahepatic cytotoxic T lymphocytes (CTL) were analyzed using major histocompatibility complex (MHC) class I tetramer and intracellular interferon (IFN)- γ staining method. Data show one representative mouse per group ($n = 3$). (b) The number of MHC tetramer⁺ CD8 lymphocytes in the liver of core (-) and core (+) mice at day 7 and day 14 following Ad-HCV-NS3 infection ($*P < 0.05$; n.s., not statistically significant). (c) The number of tetramer⁺ intracellular IFN- γ + CD8 lymphocytes in the liver of core (-) and core (+) mice at day 7 and day 14 following Ad-HCV-NS3 infection. Intrahepatic lymphocytes (IHL) were restimulated with phorbol myristate acetate (PMA)/ionophore for 5 h and IFN- γ production was determined by intracellular cytokine staining ($*P < 0.05$; n.s., not statistically significant). (d) The percentage of intracellular IFN- γ ⁺ CD8 lymphocytes in tetramer⁺ CD8 IHL of core (-) and core (+) mice on day 7 and day 14 following Ad-HCV-NS3 infection. IHL were restimulated with PMA/ionophore for 5 h and IFN- γ production was determined by intracellular cytokine staining ($*P < 0.05$; n.s., not statistically significant). □, core (-); ■, core (+).

The existence of HCV core gene cause higher expression of suppression molecules

The PD-1 and Tim-3 inhibitory pathways have been reported to play important roles in the dysfunction of effector T-cell response during viral infection. For instance, the expression of PD-1 is increased on functionally exhausted CD8 T cells during chronic viral infection.¹⁵ To investigate the relation between the viral

infectious doses or the expression of HCV core gene in the liver and suppression marker expression of antiviral CD8 IHL, we examined the expression for both PD-1 and Tim-3 in the CD8 IHL and PD-L1 in the intrahepatic APC of core (+) and core (-) following various doses Ad-HCV-NS3 infection.

We found that i.v. infection with 1×10^{10} PFU induced a significant expression of PD-1 and Tim-3 by Ad-HCV-NS3 specific intrahepatic CD8 T cells (Fig. 3).

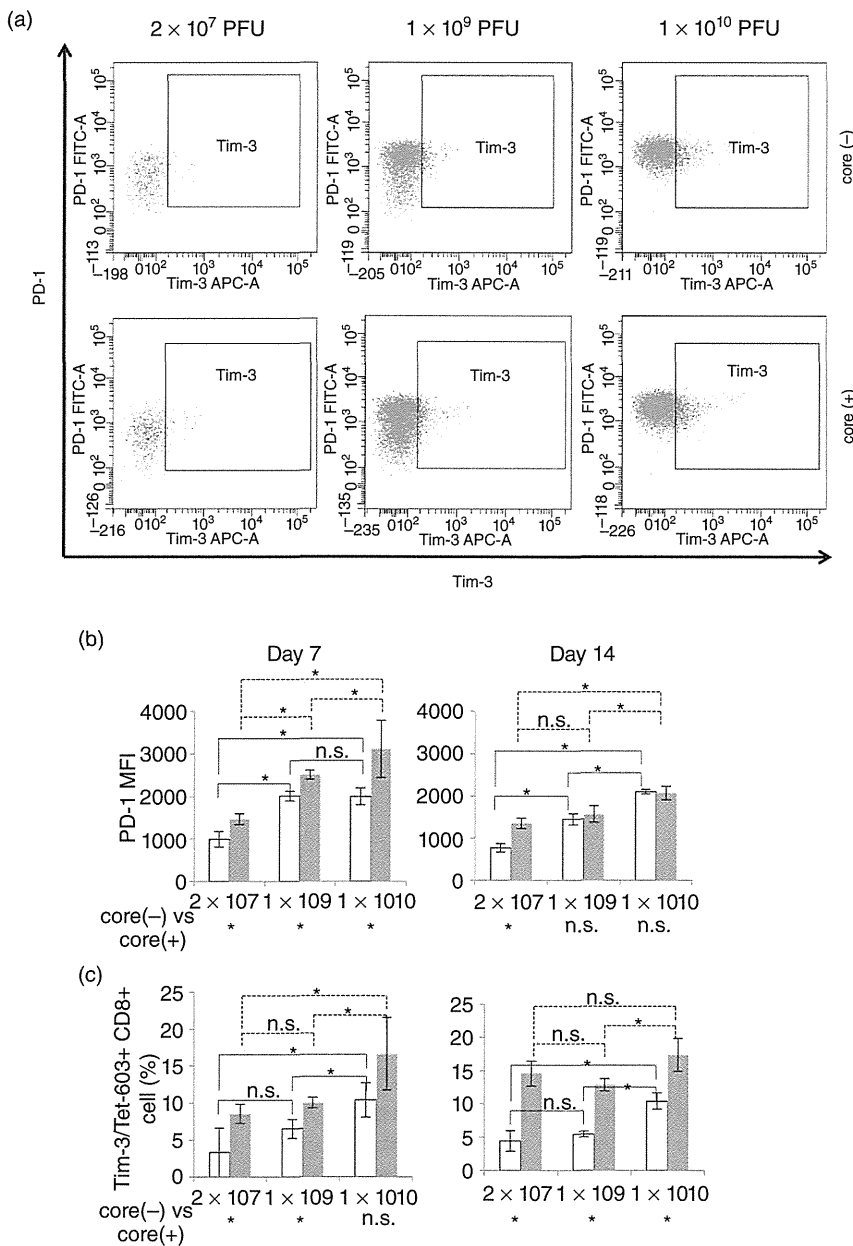


Figure 3 Differential suppression marker expression on NS3-specific CD8 lymphocyte in various infectious doses. (a) Flow cytometric dot gram gating on the hepatitis C virus (HCV)-NS3-tetramer⁺ CD8 lymphocyte at day 14 post-infection. Graded doses of adenovirus (Ad)-HCV-NS3 were administered i.v and NS3-specific intrahepatic cytotoxic T lymphocytes (CTL) were analyzed using major histocompatibility complex (MHC) class I tetramer and anti-PD-1 and anti-Tim-3 monoclonal antibody. Data show one representative mouse per group ($n=3$). (b) The median fluorescence index (MFI) value of PD-1 expressed on HCV-NS3-specific CD8 intrahepatic lymphocytes (IHL) from core (-) and core (+) mice at 14 days following Ad-HCV-NS3 infection. (* $P < 0.05$; n.s., not statistically significant). (c) The number of Tim-3⁺ HCV-NS3-specific CD8 IHL from core (-) and core (+) mice at 14 days following Ad-HCV-NS3 infection. (* $P < 0.05$; n.s., not statistically significant). □, core (-); ■, core (+).

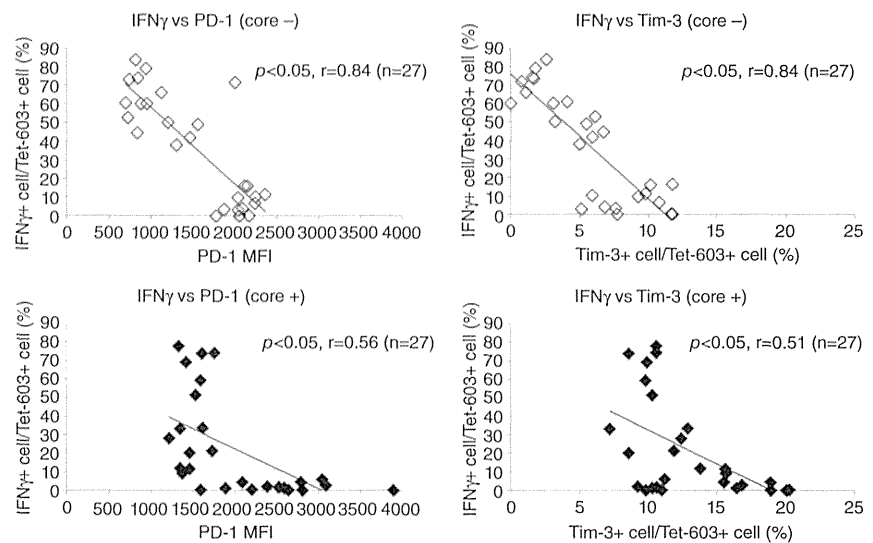


Figure 4 Inverse correlation between the percentages of interferon (IFN)- γ -producing cells and expression of regulatory molecules in antigen-specific intrahepatic CD8 T cells.

When core (+) and core (-) mice were compared, the expression of PD-1 and Tim-3 by Ad-HCV-NS3-specific intrahepatic CD8 T cells was significantly higher in core (+) than core (-) at various time points following Ad-HCV-NS3 infection. Furthermore, we found a significant inverse correlation between the percentages of IFN- γ -producing cells and expression of regulatory molecules in Ag-specific intrahepatic CD8 T cells (Fig. 4).

To determine whether suppression ligand expression by intrahepatic APC is altered in core (+) mice, the intensity of PD-L1 expressed by CD11⁺ cells was analyzed at 7 and 14 days post-infection. Intrahepatic APC showed the infectious dose-dependent augmentation of PD-L1 expression. We observed elevated expression of PD-L1 by APC in core (+) mice infected with 10^{10} PFU at both time points (Fig. 5a,b). In PD-L1 expression, we did not find a significant difference between Ad-HCV-NS3 infection and Ad ψ 5 control vector infection (Fig. 5c,d).

Taken together, these data suggest that the existence of HCV core gene suppress T-cell-mediated immune response by causing higher expression of suppression molecules.

Ag persistence after Ad-HCV-NS3 infection

To determine the Ag persistence after Ad-HCV-NS3 infection, we analyzed the expression of FLAG-tagged HCV-NS3 protein in the liver by IP-western blot after administration of 2×10^7 , 1×10^9 or 1×10^{10} PFU of the virus. The Ag expression in the liver could be found in both core (+) and core (-) mice on 21 days after

infection with 1×10^{10} PFU. When 1×10^9 PFU of Ad-HCV-NS3 was administered, HCV NS3-protein was almost cleared from the liver of core (-) mice at day 21 post-infection, whereas the Ag expression persisted in the liver of core (+) mice until day 21 post-infection (Fig. 6).

It is important to note that the loss of Ag expression in the liver of core (-) mice after infection with 1×10^9 PFU coincided with the high HCV-NS3-specific CD8 T-cell response at 14 days post-infection (Fig. 2c), whereas Ag persistence in the liver of core (+) and core (-) mice after infection with 1×10^{10} PFU was associated with strongly diminished Ag-specific CD8 T-cell response (Fig. 2c). It is likely that the expression of core protein and the high amount of Ag in the liver contributed to the functional exhaustion of HCV-NS3-specific CD8 T cells.

DISCUSSION

IN THIS STUDY, we found an impaired response of HCV-NS3-specific intrahepatic CD8 T cell in a high dose setting (1×10^{10} PFU) of Ad-HCV-NS3 infection. Furthermore, higher levels of expression of regulatory molecules, Tim-3 and PD-1, by intrahepatic CD8 T cells and PD-L1 by intrahepatic APC were observed in HCV core Tg mice and the expression increased dependent on infectious dose. In addition, we found a significant inverse correlation between the percentages of IFN- γ -producing cells and expression of regulatory molecules

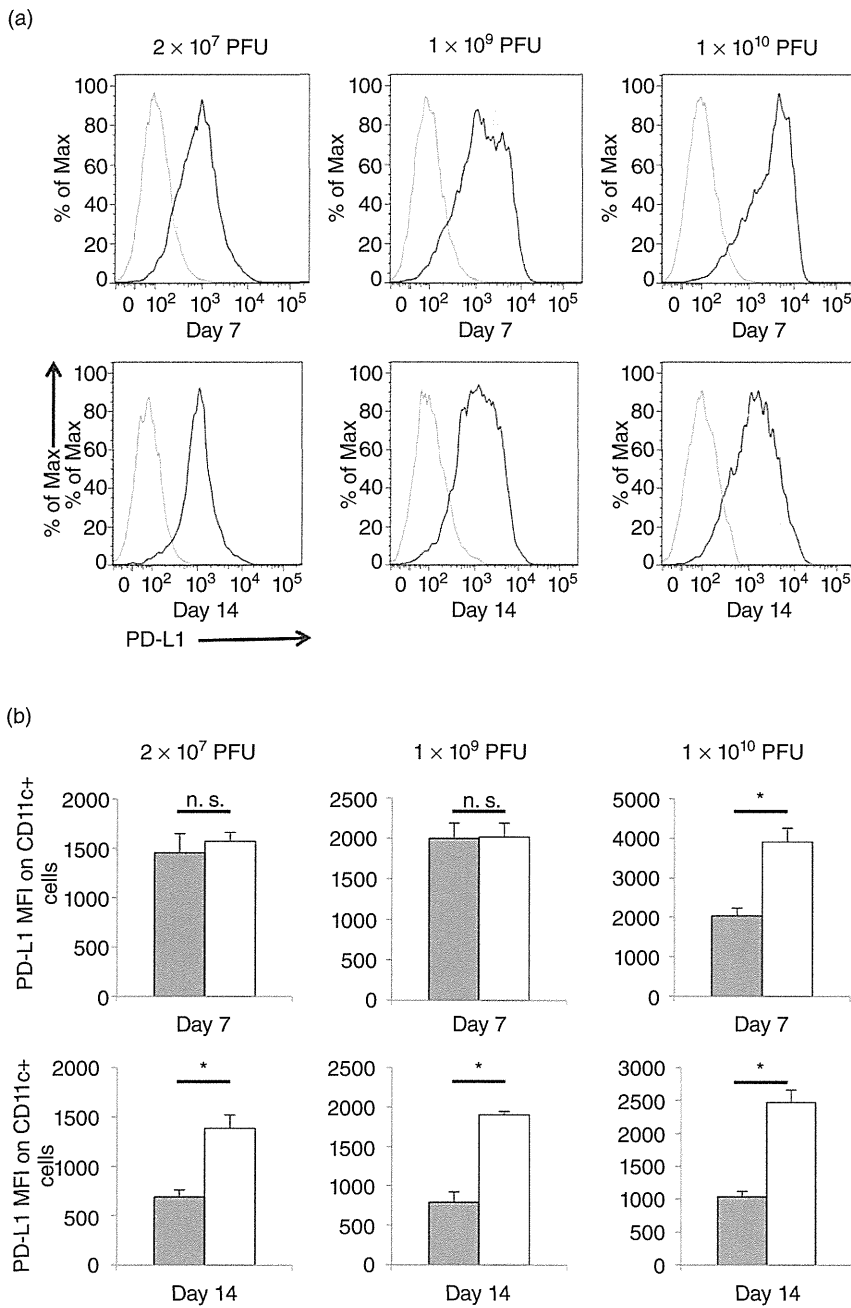


Figure 5 PD-L1 expression in the liver of core (+) and core (-) mice. Core (+) and core (-) mice were injected with 2×10^7 , 1×10^9 and 1×10^{10} plaque-forming units (PFU) of adenovirus (Ad)-hepatitis C virus (HCV)-NS3 or Ad ψ 5 control vector. (a) PD-L1 expression by intrahepatic antigen-presenting cells (APC) from core (+) and core (-) mice infected with Ad-HCV-NS3. The % of Max is the number of cells in each sample divided by the number of cells in the sample that contains the largest number of cells. (b) The median fluorescence index (MFI) expression of PD-L1 by intrahepatic CD11c⁺ leukocyte from core (+) and core (-) mice infected with Ad-HCV-NS3 (* $P < 0.05$; n.s., not statistically significant). (c) PD-L1 expression by intrahepatic APC from core (+) and core (-) mice infected with Ad-HCV-NS3 or Ad ψ 5 control vector. (d) The MFI expression of PD-L1 by intrahepatic CD11c⁺ leukocyte from core (+) and core (-) mice infected with Ad-HCV-NS3 or Ad ψ 5 control vector (n.s., not statistically significant). (a) —, isotype; ---, core (-); —, core (+); (b) ■, core (-); □, core (+); (c) —, isotype; —, Ad ψ 5; —, Ad-NS3; (d) ■, Ad ψ 5; □, Ad-NS3.

in Ag-specific intrahepatic CD8 T cells. These results indicated that high infectious dose and the presence of HCV core gene were strongly involved in ineffective CD8 T-cell responses.

Recently, a novel mechanism of T-cell dysfunction was demonstrated in a murine model of chronic LCMV infection.²⁴ It was found that the expression of PD-1 was

upregulated on dysfunctional LCMV-specific CD8 T cells in mice.²⁴ *In vivo* blockade of PD-1/PD-L1 interaction restored the functions of LCMV-specific CD8 T cells and reduced the viral titer.²⁴ More recently, other inhibitory receptors such as Tim-3 have also been studied as the factors that can cause T-cell impairments in chronic viral infections.²⁵ These influential discoveries led to

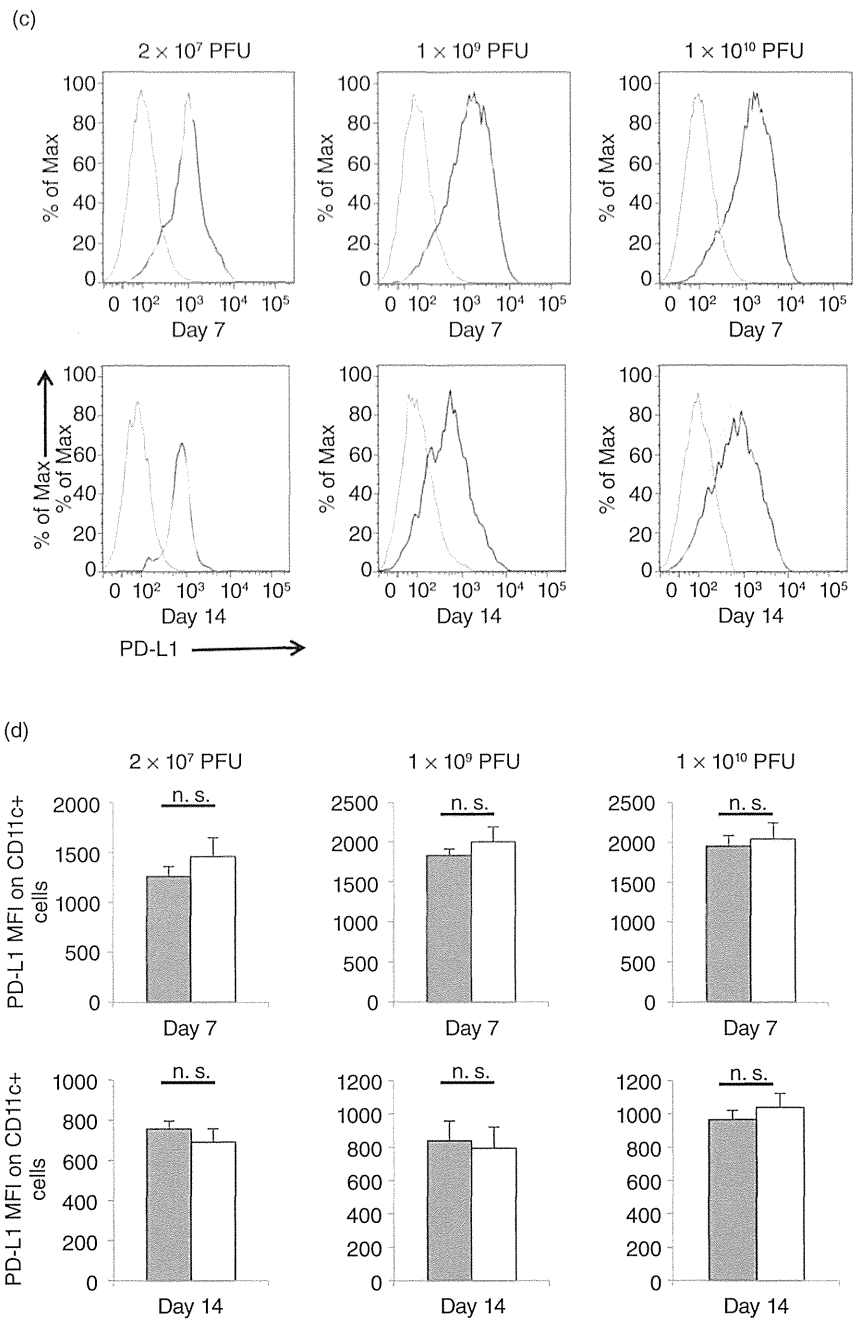


Figure 5 Continued

extensive investigations of inhibitory receptors in the regulation of T cells in human chronic viral infections.^{25,26}

Chronic HCV infection in humans is characterized by CD8 T-cell exhaustion and dysfunction.²⁷ As in chronic LCMV infection, the expression of PD-1 is similarly upregulated on the virus-specific CD8 T cells in chronic

HCV infection, and HCV-specific PD-1^{high} T cells are functionally impaired.^{28–30} Also, Tim-3 is overexpressed on HCV-specific dysfunctional CD8 T cells.²⁵ In addition, a blockade of PD-1/PD-L1 or Tim-3/galectin9 (Gal9) interaction restores T-cell functions such as proliferation, cytolytic activity and cytokine (IFN- γ and tumor necrosis factor- α) production.^{25,28–30} As was

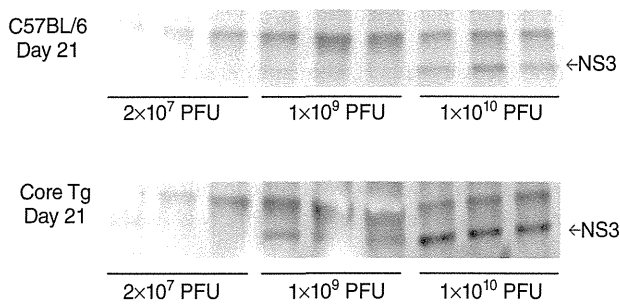


Figure 6 Persisting hepatitis C virus (HCV)-NS3 antigen detection was performed on the liver sections isolated 21 days post-infection. Liver sections were analyzed by IP-western blot assay using anti-FLAG antibody.

mentioned above, it has been reported that increased expression of inhibitory receptors is associated with the impaired HCV-specific CD8 T cells observed in chronic HCV patients. However, the underlying mechanisms for HCV-mediated impaired CD8 T-cell responses have yet to be determined. Based on our finding that lower level of activation and higher levels of expression of regulatory molecules, Tim-3 and PD-1, by intrahepatic CD8 T cells and higher levels of expression of PD-L1 by intrahepatic APC were observed in core (+) mice in comparison with core (–) mice, it is possible that HCV core-induced T-cell dysfunction is one of the viral factors that contributes to impaired CD8 T-cell responses as seen in chronic HCV patients. Our speculation is in accordance with the study by Lukens *et al.*³¹

Suppression of CTL responses via highly expressed Ag was found in chronic HCV infection. Inverse relationships between HCV viral titer and HCV-specific T cells have been reported.^{7,32,33} In this study, we found higher levels of expressions of PD-L1 by intrahepatic APC and an impaired intrahepatic CD8 T-cell response in high infectious dose setting. Moreover, we found a significant inverse correlation between the percentages of IFN- γ -producing cells and expression of regulatory molecules in Ag-specific intrahepatic CD8 T cells. It is likely that the PD-1/PD-L1 or Tim-3/Gal9 pathway play a major inhibitory role in our model. High-dose Ad-HCV NS3 infection may inhibit the NS3-specific CD8 T-cell responses not at the induction phase but at the effector phase because Ag-specific-MHC tetramer⁺ T cells were observed, and most Ag-specific MHC tetramer⁺ T cells was anergic to PMA/ionophore stimulation and these T cells expressed PD-1 and Tim-3. The role of PD-1/PD-L1 as mechanism for liver tolerance has been well established. PD-1 expression by T cells has been shown to

inhibit intrahepatic antiviral immune responses at the effector phase.^{34–36}

Hepatitis C virus infection affects approximately 170 million people in the world and is a major global health problem because infected individuals can develop liver cirrhosis and hepatocellular carcinoma. Pegylated interferon and ribavirin therapy, although beneficial in approximately half of treated patients, are expensive and associated with significant side-effects.³⁷ In this clinical context, there is an urgent need for the development of a therapeutic and/or prophylactic HCV vaccine.³⁸ Because HCV infects only humans and chimpanzees, it is difficult to evaluate effective therapeutic vaccine candidates. Recently, as a small animal model for HCV infection study, chimeric humanized mouse harboring a human hepatocyte and hematolymphoid system was established by xenotransplantation technique.^{39,40} The xenograft model provides a unique opportunity for HCV vaccine development. However, the generation of this chimeric humanized mouse requires advanced technical skills and the scarcity of adequate human primary material remains a significant logistical challenge.^{41,42} Our model showed in the present study is easy to create, and it has Ag-specific T-cell exhaustion and Ag persistent in the liver seen in chronic HCV patients. These features suggest that this system is useful for therapeutic HCV vaccine development.

ACKNOWLEDGMENTS

THIS WORK WAS supported by grants from a Saitama Medical University Internal Grant (24-A-1-01 and 24-B-1-06), Grant from Ochiai Memorial Award 2011 and the Ministry of Health, Labor, and Welfare, Japan. The authors thank Hiroe Akatsuka for technical assistance.

REFERENCES

- 1 Shepard CW, Finelli L, Alter MJ. Global epidemiology of hepatitis C virus infection. *Lancet Infect Dis* 2005; 5: 558–67.
- 2 Kamal SM. Acute hepatitis C: a systematic review. *Am J Gastroenterol* 2008; 103: 1283–97.
- 3 Alter HJ, Seeff LB. Recovery, persistence, and sequelae in hepatitis C virus infection: a perspective on long-term outcome. *Semin Liver Dis* 2000; 20: 17–35.
- 4 Grüner NH, Gerlach TJ, Jung MC *et al.* Association of hepatitis C virus-specific CD8⁺ T cells with viral clearance in acute hepatitis C. *J Infect Dis* 2000; 181: 1528–36.

- 5 Chang KM, Reherrmann B, McHutchison JG *et al.* Immunological significance of cytotoxic T lymphocyte epitope variants in subjects chronically infected by the hepatitis C virus. *J Clin Invest* 1997; 100: 2376–85.
- 6 Lechmann M, Woitas RP, Langhans B *et al.* Decreased frequency of HCV core-specific peripheral blood mononuclear cells with type 1 cytokine secretion in chronic hepatitis. *Can J Hepatol* 1999; 31: 971–8.
- 7 Reherrmann B, Chang KM, McHutchison JG *et al.* Differential cytotoxic T-lymphocyte responsiveness to the hepatitis B and C viruses in chronically infected patients. *J Virol* 1996; 70: 7092–102.
- 8 Wedemeyer H, He XS, Nascimbeni M *et al.* Impaired effector function of hepatitis C virus specific CD8+ T cells in chronic hepatitis C virus infection. *J Immunol* 2002; 169: 3447–58.
- 9 Zinkernagel RM, Hengartner H. Regulation of the immune response by antigen. *Science* 2001; 293: 251–3.
- 10 Moskophidis D, Lechner F, Pircher H, Zinkernagel RM. Virus persistence in acutely infected immunocompetent mice by exhaustion of antiviral cytotoxic effector T cells. *Nature* 1993; 362: 758–61.
- 11 Wherry EJ, Blattman JN, Murali-Krishna K, van der Most R, Ahmed R. Viral persistence alters CD8 T-cell immunodominance and tissue distribution and results in distinct stages of functional impairment. *J Virol* 2003; 77: 4911–27.
- 12 Zajac AJ, Blattman JN, Murali-Krishna K *et al.* Viral immune evasion due to persistence of activated T cells without effector function. *J Exp Med* 1998; 188: 2205–13.
- 13 Wherry EJ, McElhaugh MJ, Eisenlohr LC. Generation of CD8 T cell memory in response to low, high, and excessive levels of epitope. *J Immunol* 2002; 168: 4455–61.
- 14 Eisen-Vandervelde AL, Waggoner SN, Yao ZQ, Cale EM, Hahn CS, Hahn YS. Hepatitis C virus core selectively suppresses interleukin-12 synthesis in human macrophages by interfering with AP-1 activation. *J Biol Chem* 2004; 279: 43479–86.
- 15 Watanabe T, Bertoletti A, Tanoto TA. PD1/PD-L1 pathway and T-cell exhaustion in chronic hepatitis virus infection. *J Viral Hepat* 2010; 17: 453–8.
- 16 Yao ZQ, Eisen-Vanderveld A, Waggoner SN, Cale EM, Hahn YS. Direct binding of hepatitis C virus core to gC1qR on CD4+ and CD8+ T cells leads to impaired activation of Lck and Akt. *J Virol* 2004; 78: 6409–19.
- 17 Yao ZQ, Nguyen DT, Hiotellis AI, Hahn YS. Hepatitis C virus core protein inhibits human T lymphocyte responses by a complement-dependent regulatory pathway. *J Immunol* 2001; 167: 5264–72.
- 18 Cavanaugh VL, Guidotti LG, Chisari FV. Inhibition of hepatitis B virus replication during adenovirus and cytomegalovirus infections in transgenic mice. *J Virol* 1998; 72: 2630–7.
- 19 von Freyend MJ, Untergasser A, Arzberger S *et al.* Sequential control of hepatitis B virus in a mouse model of acute, self-resolving hepatitis B. *J Viral Hepat* 2011; 18: 216–26.
- 20 Moriya K, Yotsuyanagi H, Shintani Y *et al.* Hepatitis C virus core protein induces hepatic steatosis in transgenic mice. *J Gen Virol* 1997; 78: 1527–31.
- 21 Koike K, Moriya K, Ishibashi K *et al.* Sialadenitis histologically resembling Sjogren syndrome in mice transgenic for hepatitis C virus envelope genes. *Proc Natl Acad Sci U S A* 1997; 94: 233–6.
- 22 Kolykhalov AA, Agapov EV, Blight KJ, Mihalik K, Feinstone SM, Rice CM. Transmission of hepatitis C by intrahepatic inoculation with transcribed RNA. *Science* 1997; 277: 570–4.
- 23 Frelin L, Alheim M, Chen A *et al.* Low dose and gene gun immunization with a hepatitis C virus nonstructural (NS) 3 DNA-based vaccine containing NS4A inhibit NS3/4A-expressing tumors in vivo. *Gene Ther* 2003; 10: 686–99.
- 24 Barber DL, Wherry EJ, Masopust D *et al.* Restoring function in exhausted CD8 T cells during chronic viral infection. *Nature* 2006; 439: 682–7.
- 25 Golden-Mason L, Palmer BE, Kassam N *et al.* Negative immune regulator Tim-3 is overexpressed on T cells in hepatitis C virus infection and its blockade rescues dysfunctional CD4+ and CD8+ T cells. *J Virol* 2009; 83: 9122–30.
- 26 Sharpe AH, Wherry EJ, Ahmed R, Freeman GJ. The function of programmed cell death 1 and its ligands in regulating autoimmunity and infection. *Nat Immunol* 2007; 8: 239–45.
- 27 Spangenberg HC, Viazov S, Kersting N *et al.* Intrahepatic CD8+ T-cell failure during chronic hepatitis C virus infection. *Hepatology* 2005; 42: 828–37.
- 28 Golden-Manson L, Palmer B, Klarquist J, Mengshol JA, Castelblanco N, Rosen HR. Upregulation of PD-1 expression on circulating and intrahepatic hepatitis C virus-specific CD8+ T cells associated with reversible immune dysfunction. *J Virol* 2007; 81: 9249–58.
- 29 Penna A, Pilli M, Zerbini A *et al.* Dysfunction and functional restoration of HCV-specific CD8 responses in chronic hepatitis C virus infection. *Hepatology* 2007; 45: 588–601.
- 30 Radziewicz H, Ibegbu CC, Fernandez ML *et al.* Liver-infiltrating lymphocytes in chronic human hepatitis C virus infection display an exhausted phenotype with high levels of PD-1 and low levels of CD127 expression. *J Virol* 2007; 81: 2545–53.
- 31 Lukens JR, Cruise MW, Lassen MG, Hahn YS. Blockade of PD-1/B7-H1 interaction restores effector CD8+ T cell responses in a hepatitis C virus core murine model. *J Immunol* 2008; 180: 4875–84.
- 32 Sreekumar R, Gonzalez-Koch A, Maor-Kendler Y *et al.* Early identification of recipient with progressive histologic recurrence of hepatitis C after liver transplantation. *Hepatology* 2000; 32: 1125–30.

- 33 Sugimoto K, Ikeda F, Standanlick J, Frederick A, Alter HJ, Chang KM. Suppression of HCV-specific T cells without differential hierarchy demonstrated *ex vivo* in persistent HCV infection. *Hepatology* 2003; 38: 1437–48.
- 34 Isogawa M, Furuichi Y, Chisaki FV. Oscillating CD8+ T cell effector functions after antigen recognition in the liver. *Immunity* 2005; 23: 53–63.
- 35 Iwai Y, Terawaki S, Ikegawa M, Okazaki T, Honjo T. PD-1 inhibits antiviral immunity at the effector phase in the liver. *J Exp Med* 2003; 198: 39–50.
- 36 Maier H, Isogawa M, Freeman GJ, Chisari FV. PD-1:PD-L1 interactions contribute to the functional suppression of virus-specific CD8+ T lymphocytes in the liver. *J Immunol* 2007; 178: 2714–20.
- 37 Pawlotsky JM. Therapy of hepatitis C: from empiricism to eradication. *Hepatology* 2006; 43: S207–20.
- 38 Callendret B, Walker C. A siege of hepatitis: immune boost for viral hepatitis. *Nature Med* 2011; 17: 252–3.
- 39 Legrand N, Ploss A, Balling R *et al.* Humanized mice for modeling human infectious disease: challenges, progress, and outlook. *Cell Host Microb* 2009; 6: 5–9.
- 40 Robinet E, Baumert TF. A first step towards a mouse model for hepatitis C virus infection containing a human immune system. *J Hepatol* 2011; 55: 718–20.
- 41 Kimura K, Kohara M. An experimental mouse model for hepatitis C virus. *Exp Anim* 2011; 60: 93–100.
- 42 Ploss A, Rice CM. Towards a small animal model for hepatitis C. *EMBO Rep* 2009; 10: 1220–7.

Clinical characteristics, treatment, and prognosis of non-B, non-C hepatocellular carcinoma: a large retrospective multicenter cohort study

Ryosuke Tateishi · Takeshi Okanoue · Naoto Fujiwara ·
Kiwamu Okita · Kendo Kiyosawa · Masao Omata ·
Hiromitsu Kumada · Norio Hayashi · Kazuhiko Koike

Received: 2 April 2014 / Accepted: 2 June 2014
© The Author(s) 2014. This article is published with open access at Springerlink.com

Abstract

Background The number of hepatocellular carcinoma (HCC) patients with non-viral etiologies is increasing in Japan. We conducted a nation-wide survey to examine the characteristics of those patients.

Methods After we assessed the trend of patients who were first diagnosed with HCC at 53 tertiary care centers in Japan from 1991 to 2010, we collected detailed data of 5326 patients with non-viral etiology. The etiologies were

categorized as autoimmune hepatitis, primary biliary cirrhosis, alcoholic liver disease (ALD), non-alcoholic fatty liver disease (NAFLD), unclassified, and other. Baseline characteristics at initial diagnosis, the modality of the initial treatment, and survival status were collected via a website. Survival of the patients was assessed by the Kaplan–Meier method and Cox proportional hazard regression.

Results The proportion of patients with non-viral etiologies increased from 10.0 % in 1991 to 24.1 % in 2010. Of the patients, 92 % were categorized as ALD, NAFLD, or unclassified. Body mass index (BMI) was ≥ 25 kg/m² in 39 %. Diabetes was most prevalent in NAFLD (63 %), followed by unclassified etiology (46 %) and ALD (45 %). Approximately 80 % of patients underwent radical therapy, including resection, ablation, or transarterial chemoembolization. Survival rates at 3, 5, 10, 15, and 20 years were 58.2, 42.6, 21.5, 15.2, and 15.2 %, respectively. Multivariate analysis revealed that patients with BMI > 22 and ≤ 25 kg/m² showed the best prognosis versus other BMI categories, after adjusting by age, gender, tumor-related factors, and Child-Pugh score.

Conclusions Most cases of non-B, non-C HCC are related to lifestyle factors, including obesity and diabetes. Slightly overweight patients showed the best prognosis.

Keywords Hepatocellular carcinoma · Non-alcoholic fatty liver disease · Non-alcoholic steatohepatitis · Alcoholic liver disease · Retrospective study

For the INUYAMA NOBLESSE Study group. Members of the INUYAMA NOBLESSE Study group are listed in “Appendix”.

Electronic supplementary material The online version of this article (doi:10.1007/s00535-014-0973-8) contains supplementary material, which is available to authorized users.

R. Tateishi (✉) · N. Fujiwara · K. Koike
Department of Gastroenterology, Graduate School of Medicine,
The University of Tokyo, 7-3-1 Hongo, Bunkyo-ku,
Tokyo 113-8655, Japan
e-mail: tateishi-ty@umin.ac.jp

T. Okanoue
Saiseikai Suita Hospital, Suita, Japan

K. Okita
Ajisu Kyoritsu Hospital, Yamaguchi, Japan

K. Kiyosawa
Shironishi Hospital, Matsumoto, Japan

M. Omata
Yamanashi Prefectural Hospital Organization, Kofu, Japan

H. Kumada
Toranomom Hospital, Tokyo, Japan

N. Hayashi
Kansai Rosai Hospital, Amagasaki, Japan

Introduction

Hepatocellular carcinoma (HCC) is a typical example of an infection-associated malignancy [1]. The geographical

distribution of the highly endemic area of HCC overlaps that of chronic hepatitis B and C [2]. Rigorous efforts to control horizontal transmission of hepatitis B virus (HBV) by vaccination since the mid-1980s succeeded in reducing hepatitis B-related HCC in children [3]. Screening for hepatitis C virus (HCV) and the ending of paid blood donations markedly reduced the incidence of transfusion-associated hepatitis [4]. In those with active chronic hepatitis B, long-term suppression using nucleotide analogs may reduce the incidence of HBV-related HCC [5, 6], and the eradication of HCV by interferon-based therapy can reduce HCV-related HCC [7, 8]. It can reasonably be concluded that hepatitis virus-related HCC will continue to decrease in the future [9, 10].

While HCC is a typical example of a virus-related cancer, it is also well known to be strongly related to life style. Chronic alcoholism is a classical risk factor [11]; more recently, obesity has been recognized to strongly affect HCC development in males, versus various other malignancies [12]. There is also growing evidence suggesting that type 2 diabetes increases the incidence of HCC [13, 14]. Due to the globally increasing proportion of the obese population over the past 30 years [15], obesity-related HCC will likely continue to increase.

Unlike virus-related HCC, in which the high-risk populations and surveillance programs are well established, little is known about the characteristics of virus-unrelated HCC. To reduce the forthcoming global burden of obesity-related HCC, to clarify its clinical features is quite important. The Non-B, Non-C Liver Cancer, Etiology, Prognosis and Treatment (NOBLESSE) study was conducted as a special project of the Inuyama Symposium, an assembly of 56 gastroenterology and hepatology units in university hospitals and tertiary care hospitals in Japan, to investigate the characteristics of non-B, non-C HCC patients.

Patients and methods

Patients

This retrospective study complied with the ethical guidelines for epidemiological research designed by the Japanese Ministry of Education, Culture, Sports, Science and Technology and Ministry of Health, Labour, and Welfare. The study protocol was approved by the University of Tokyo Medical Research Center Ethics Committee (approval number 3710) and the Institutional Review Board or Ethics Committee of each participating institution. Informed consent was waived because of the retrospective design. This study was registered with the University Hospital Medical Information Network (UMIN) Clinical Trial Registry (UMIN-CTR000007570).

First we collected the number of patients with HCC who were first diagnosed with HCC in the participating hospitals from 1991 to 2010 and categorized them as HBV-related, HCV-related, both HBV and HCV-related, and non-B, non-C to assess trends in the proportion of background etiologies. Next we collected detailed data of non-B, non-C HCC patients defined as negative for both hepatitis B surface antigen (HBsAg) and anti-HCV antibody. Patients who lost HBsAg before the diagnosis of HCC or who were positive for HBV DNA were excluded.

Diagnosis of HCC

The diagnosis of HCC was made by dynamic computed tomography (CT) or dynamic magnetic resonance imaging (MRI) with consideration of hyperattenuation in the arterial phase, with washout in the late phase as a definite sign of this disease [16] or pathology. In years when dynamic CT was not available, the diagnosis was also made by angiography.

Data collection

The patients were registered via a website specially designed by the investigators. The following characteristics at diagnosis were collected: age, gender, body height, body weight, etiology of background liver disease, daily alcohol consumption; comorbidities including liver cirrhosis, fatty liver by ultrasonography, hypertension, dyslipidemia, and diabetes; tumor factors including tumor size of the maximal nodule, number of tumor nodules, the presence of vascular invasion, and extrahepatic metastasis; symptoms including ascites and hepatic encephalopathy, laboratory data, including serum albumin, total bilirubin, aspartate aminotransferase (AST), alanine aminotransferase (ALT), alkaline phosphatase (ALP), gamma-glutamyl transpeptidase (GGT), platelet count, prothrombin activity, alpha-fetoprotein (AFP), des-gamma-carboxyprothrombin (DCP), and lens culinaris agglutinin-reactive fraction of AFP (AFP-L3); and treatment modality for the first time, including hepatic resection, liver transplantation, ablation, transarterial chemoembolization (TACE), transarterial chemotherapy, systemic chemotherapy, radiation therapy, and supportive therapy. Body mass index (BMI), Child–Turcotte–Pugh (CTP) score, and Barcelona–Clinic–Liver–Cancer (BCLC) stages were calculated automatically using the data obtained above.

The etiology of background liver diseases was categorized as follows: autoimmune hepatitis (AIH), primary biliary cirrhosis (PBC), AIH–PBC overlap syndrome, alcoholic liver disease, non-alcoholic fatty liver disease (NAFLD), Budd–Chiari syndrome, hemochromatosis, Wilson disease, and others. The diagnosis of the

background liver disease, hypertension, dyslipidemia, and diabetes was made by the attending physician, based on the Japanese clinical guidelines for each disease. Daily alcohol consumption was calculated from forms of alcohol and frequency. Alcoholic liver disease was defined as chronic liver injury with daily alcohol consumption ≥ 80 g/day without another definite etiology. NAFLD was defined as a history of fatty liver or who were diagnosed with fatty liver, radiologically or pathologically, with alcohol consumption ≤ 20 g/day. Those with cryptogenic chronic liver disease who did not meet the criteria described above for alcoholic liver disease or NAFLD were categorized as unclassified.

Patient survival status was also registered. Status was defined as alive, dead, or lost to follow-up. Observations were censored on 31 December 2011. In diseased patients, the cause of death was categorized according to the criteria of the Liver Cancer Study Group of Japan [17], as follows: liver cancer progression, liver failure, gastrointestinal bleeding, gastro-esophageal varices rupture, rupture of liver cancer, operative death, other, and unknown.

Statistical analysis

Data are expressed as medians with 25th to 75th percentiles, unless otherwise indicated. Numbers and percentages were used for qualitative variables. Student's *t* test was used for comparisons of two continuous variables. Differences among groups were assessed with one-way analysis of variance (ANOVA) for continuous data, and with the Chi squared test for categorical data. The Cochran–Armitage trend test was used to evaluate increasing or decreasing trends in etiology. Survival time was defined as the interval between the day of the first diagnosis and death or the last visit to the hospital until 31 December 2011. Cumulative survival curves were constructed with the Kaplan–Meier method and compared with the log-rank test. To assess the hazard ratios of various factors on overall survival, the Cox proportional hazard model was used.

Statistical analyses were performed using the 'R' software (ver. 2.13.0; <http://www.R-project.org>). All tests were two-sided, and *p* values < 0.05 were considered to indicate statistical significance.

Results

Patient profiles

Of 33,782 patients who were first diagnosed with HCC at the 53 participating hospitals from 1991 to 2010, 5326 (15.8 %) were categorized as non-B, non-C. A marked

increase in the proportion of patients categorized as non-B, non-C was observed ($p < 0.001$ by Cochran–Armitage test; Fig. 1). The proportion of non-B, non-C patients was 24.1 % in 2010, whereas it was only 10.0 % in 1991. The distribution of background liver diseases among non-B, non-C patients was as follows: AIH in 161 (3.0 %), PBC in 164 (3.1 %), AIH–PBC overlap syndrome in 18 (0.3 %), alcoholic liver disease in 1423 (26.7 %), NAFLD in 596 (11.2 %), Budd-Chiari Syndrome in 20 (0.4 %), hemochromatosis in 9 (0.2 %), Wilson's disease in 5 (0.1 %), unclassified in 2875 (54.0 %), and other in 53 (1.0 %). 'Other' included schistosomiasis japonica, suspicion of autoimmune liver diseases, and normal liver. As few patients were categorized as AIH–PBC overlap syndrome, Budd-Chiari syndrome, hemochromatosis and Wilson's disease, they were combined with 'others' in Table 1. Among non-B, non-C patients, 31 and 10 % were diagnosed as HCC at the department of gastroenterology or hepatology and other department in the participating hospital, respectively. The remaining 59 % were diagnosed at other hospitals and referred to the participating hospitals. Forty-one percent of patients were followed by imaging modalities before the diagnosis of HCC.

The median [interquartile range (IQR)] age in the entire cohort was 70.0 (63.0–75.0) years and approximately three-quarters were males. Patients with alcoholic liver disease were significantly younger than other etiologies ($p < 0.001$). The male to female ratio was different among the etiologies: females predominated in autoimmune liver diseases. The vast majority were non drinkers or light drinkers, except for those with alcoholic liver disease or unclassified etiology. Among those judged as unclassified, 41 % were moderate drinkers.

The distribution of BMI varied across the etiologies and gender. The median BMI was the highest in those with

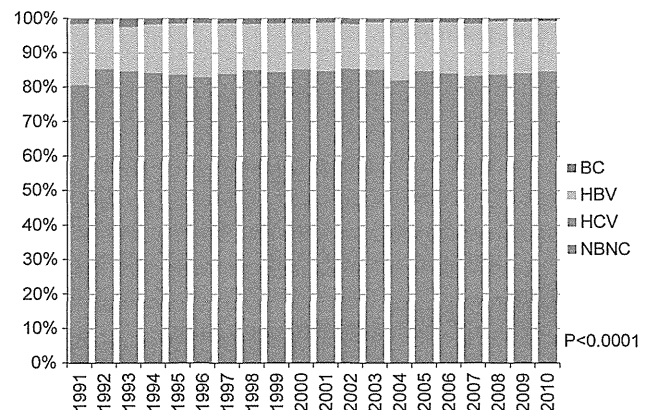


Fig. 1 Trend in background liver disease in hepatocellular carcinoma in Japan. A marked increase in the proportion of patients categorized as non-B, non-C in the participating hospitals was observed ($p < 0.001$ by Cochran–Armitage test)

Table 1 Baseline characteristics of the HCC patients analyzed in this study ($n = 5,326$)

	ALL	AIH	PBC	Alcoholic liver disease	NAFLD	Unclassified	Others
Number of patients	5,326	161	166	1,423	596	2,875	105
Age (year)							
Median	70.0	70.0	71.5	66.0	72.0	71.0	70.0
IQR	63.0–75.0	66.0–76.0	66.0–77.0	60.0–72.0	66.0–77.0	64.0–76.0	58.0–76.0
Male gender [n (%)]	4,022 (75.5)	43 (26.7)	52 (31.3)	1,327 (93.3)	348 (58.4)	2,188 (76.1)	64 (61.0)
Alcohol consumption (g/day) ^a							
≤ 20 [n (%)]	2623 (50.9)	144 (90.0)	146 (90.7)		596 (100.0)	1661 (59.0)	80 (86.0)
21–79 [n (%)]	1179 (22.9)	9 (5.6)	9 (5.6)			1154 (41.0)	7 (7.5)
≥ 80 [n (%)]	1351 (26.2)	7 (3.7)	6 (3.7)	1423 (100.0)			6 (6.5)
Diabetes [n (%)] ^b	2345 (46.1)	48 (30.6)	27 (17.0)	621 (45.2)	359 (62.7)	1264 (46.4)	26 (27.1)
Hypertension [n (%)] ^c	2063 (42.7)	51 (35.4)	42 (26.8)	493 (38.0)	313 (55.5)	1135 (44.1)	29 (31.9)
Dyslipidemia [n (%)] ^d	720 (14.6)	26 (17.1)	12 (7.6)	171 (12.7)	125 (22.9)	374 (14.2)	12 (12.6)
Fatty liver [n (%)] ^e	936 (24.0)	18 (15.5)	7 (5.5)	219 (20.7)	280 (64.4)	403 (19.3)	9 (13.4)
Liver Cirrhosis [n (%)] ^f	3439 (67.0)	127 (80.9)	145 (87.9)	1115 (80.2)	368 (63.4)	1619 (59.0)	65 (67.0)
Anti-HBcAb positive [n (%)] ^g	1501 (40.3)	27 (23.5)	35 (31.3)	410 (40.8)	159 (34.6)	837 (43.0)	33 (40.7)
ALT (U/L)							
Median	32	29	29	33	33	32	29
IQR	22–50	20–44	20–41.3	22–50	22–51	22–51	20–54
Platelet count ($\times 10^9/\mu\text{L}$) ^h							
Median	135	105	103	123	138	148	124
IQR	90–193	72–166	74–139	84–173	94–189	97–205	81–183
Child-Pugh class ⁱ							
A [n (%)]	3500 (69.0)	89 (57.4)	83 (52.9)	843 (62.1)	439 (76.5)	1976 (72.4)	70 (72.2)
B [n (%)]	1231 (24.3)	54 (34.8)	57 (36.3)	383 (28.2)	120 (20.9)	595 (21.8)	22 (22.7)
C [n (%)]	338 (6.7)	12 (7.7)	17 (10.8)	131 (9.7)	15 (2.6)	158 (5.8)	5 (5.2)
Tumor characteristics							
Maximal tumor size (cm) ^j							
Median	3.2	3.0	2.8	3.0	3.0	3.5	3.0
IQR	2.0–6.0	2.0–4.3	1.7–3.5	2.0–5.0	2.0–5.0	2.2–7.0	2.0–5.1
Diffuse type [n (%)]	209 (4.0)	6 (3.7)	1 (0.6)	62 (4.4)	17 (2.9)	119 (4.2)	4 (3.8)
Number of nodules ^k							
Single [n (%)]	2700 (51.1)	87 (54.0)	110 (66.3)	664 (46.8)	340 (57.0)	1443 (50.8)	56 (53.8)
2–3 [n (%)]	1368 (25.9)	46 (28.6)	40 (24.1)	402 (28.3)	156 (26.2)	697 (24.5)	27 (26.0)
> 3 [n (%)]	1220 (23.1)	28 (17.4)	16 (9.6)	353 (24.9)	100 (16.8)	702 (24.7)	21 (20.2)
Vascular invasion [n (%)] ^l	187 (3.5)	3 (1.9)	1 (0.6)	52 (3.7)	13 (2.2)	116 (4.1)	2 (1.9)
Extrahepatic metastasis [n (%)] ^m	401 (7.6)	8 (5.0)	2 (1.2)	114 (8.0)	26 (4.4)	244 (8.6)	7 (6.7)
AFP (ng/mL) ⁿ							
≤ 20 [n (%)]	2908 (59.4)	80 (54.1)	71 (51.4)	827 (62.4)	361 (63.1)	1515 (58.0)	54 (55.7)
21–200 [n (%)]	820 (16.8)	33 (22.3)	29 (21.0)	229 (17.3)	92 (16.1)	423 (16.2)	14 (14.4)
> 200 [n (%)]	1164 (23.8)	35 (23.6)	38 (27.5)	270 (20.4)	119 (20.8)	673 (25.8)	29 (29.9)
DCP (mAU/mL) ^o							
≤ 100 [n (%)]	2121 (45.8)	75 (53.6)	81 (59.1)	593 (46.8)	299 (53.9)	1032 (42.1)	41 (47.7)
101–400 [n (%)]	787 (17.0)	23 (16.4)	25 (18.2)	227 (17.9)	95 (17.1)	400 (16.3)	17 (19.8)
> 400 [n (%)]	1727 (37.3)	42 (30.0)	31 (22.6)	448 (35.3)	161 (29.0)	1017 (41.5)	28 (32.6)
AFP-L3 (%) ^p							
≤ 10 [n (%)]	1765 (67.7)	53 (64.6)	39 (55.7)	498 (69.6)	263 (73.5)	881 (66.1)	31 (66.0)
10.1–15 [n (%)]	74 (2.8)	3 (3.7)	4 (5.7)	17 (2.4)	7 (2.0)	43 (3.2)	0 (0)
> 15 [n (%)]	767 (29.4)	26 (31.7)	27 (38.6)	201 (28.1)	88 (24.6)	409 (30.7)	16 (34.0)

As few patients were categorized as having the AIH–PBC overlap syndrome, Budd–Chiari syndrome, hemochromatosis or Wilson’s disease, they were combined with ‘others’. Data were missing in ^a173, ^b241, ^c498, ^d388, ^e1434, ^f193, ^g1606, ^h61, ⁱ257, ^j42, ^k38, ^l28, ^m26, ⁿ434, ^o691, and ^p3677 patients. AFP alpha-fetoprotein, AFP-L3 lens culinaris agglutinin-reactive fraction of AFP, ALT alanine aminotransferase, Anti-HBcAb anti-hepatitis B core antibody, DCP des-gamma-carboxy prothrombin, IQR interquartile range

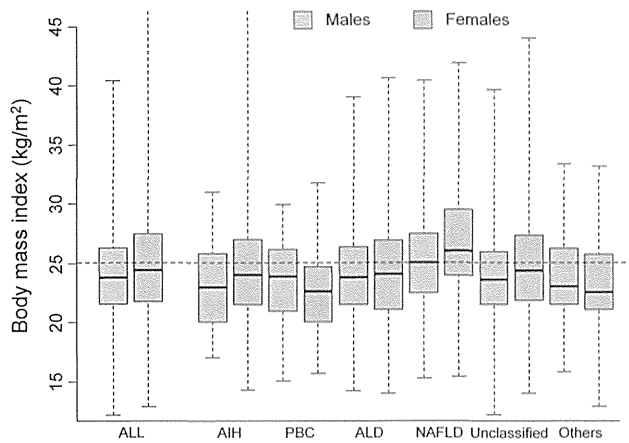


Fig. 2 Body mass index according to background liver disease. Median (25th–75th percentiles) BMI values in all categories were 23.8 (21.6–26.3) kg/m² in males and 24.4 (21.8–27.5) kg/m² in females. Box plot ‘whiskers’ show the minimum and maximum values; the horizontal line in each box plot shows the median, and the colored segment shows the interquartile range. AIH autoimmune hepatitis, PBC primary biliary cirrhosis, ALD alcoholic liver disease, NAFLD non-alcoholic fatty liver disease

NAFLD. Females had significantly higher BMI than males in NAFLD and those unclassified ($p = 0.01$ and <0.001 , respectively; Fig. 2).

Nearly half of the patients were complicated with diabetes (Table 1, Supplementary Fig. 1). The proportion of those with diabetes was highest in NAFLD patients. A similar trend was observed in the proportions of hypertension and dyslipidemia. The presence of fatty liver, judged by ultrasonography at the diagnosis of HCC, varied across the etiologies. The proportion was approximately 20 % in alcoholic liver disease and unclassified etiology, while it was lower in autoimmune liver diseases, especially PBC. It was also suggested that fatty liver could not be detected by ultrasonography in approximately 30 % at the diagnosis of HCC in NAFLD.

Approximately two-thirds of the patients were complicated with cirrhosis. The proportion of those with cirrhosis was lower in those with NAFLD and unclassified etiology compared with other etiologies ($p < 0.001$). Reflecting the proportion of cirrhosis, platelet counts were highest in those with unclassified etiology, followed by those with NAFLD.

Regarding the diagnosis process, 30.3 % of the patients had their tumor pointed out for the first time in the participating department, 10.6 % in another department of the same hospital, and 59.1 % at other hospitals. Patients were diagnosed at more advanced stages in those with unclassified etiology; the tumor size was the largest and the proportion of patients with vascular invasion and extrahepatic metastasis was also the largest. The sensitivity of DCP was superior to that of AFP (54.2 vs. 40.6 % with

cutoff values of 100 mAU/mL and 20 ng/mL, respectively).

Treatment and survival

Among 5058 patients in whom BCLC staging could be determined, 2533 (50.1 %), 1913 (37.8 %), 283 (5.6 %), and 329 (6.5 %) were categorized as stages A, B, C, and D, respectively (Table 2). The distribution of the initial treatment was as follows: resection in 1073 (20.3 %), ablation in 1060 (20.0 %), TACE + ablation in 470 (8.9 %), TACE in 1590 (30.1 %), transarterial chemotherapy with one-shot and continuous infusion in 99 (1.9 %), systemic therapy in 20 (0.3 %), radiation therapy in 20 (0.4 %), liver transplantation in 17, others in 30 (0.6 %), and supportive care in 429 (8.1 %).

During the mean follow-up period of 2.6 years, 2225 patients died and 670 patients were lost to follow-up. The causes of death were cancer progression in 1411 (58.0 %), liver failure in 359 (14.8 %), gastrointestinal bleeding, including varices rupture, in 87 (3.6 %), tumor rupture in 71 (2.9 %), operative death in 13 (0.5 %), and other in 284 (11.7 %). The cause of death was unspecified in 206 (8.5 %). Median survival time [95 % confidence interval (CI)] after the initial diagnosis of HCC was 4.03 (3.82–4.20) years. Overall survival rates at 1, 3, 5, 7, 10, 15, and 20 years were 80.1, 58.2, 42.6, 32.2, 21.5, 15.2,

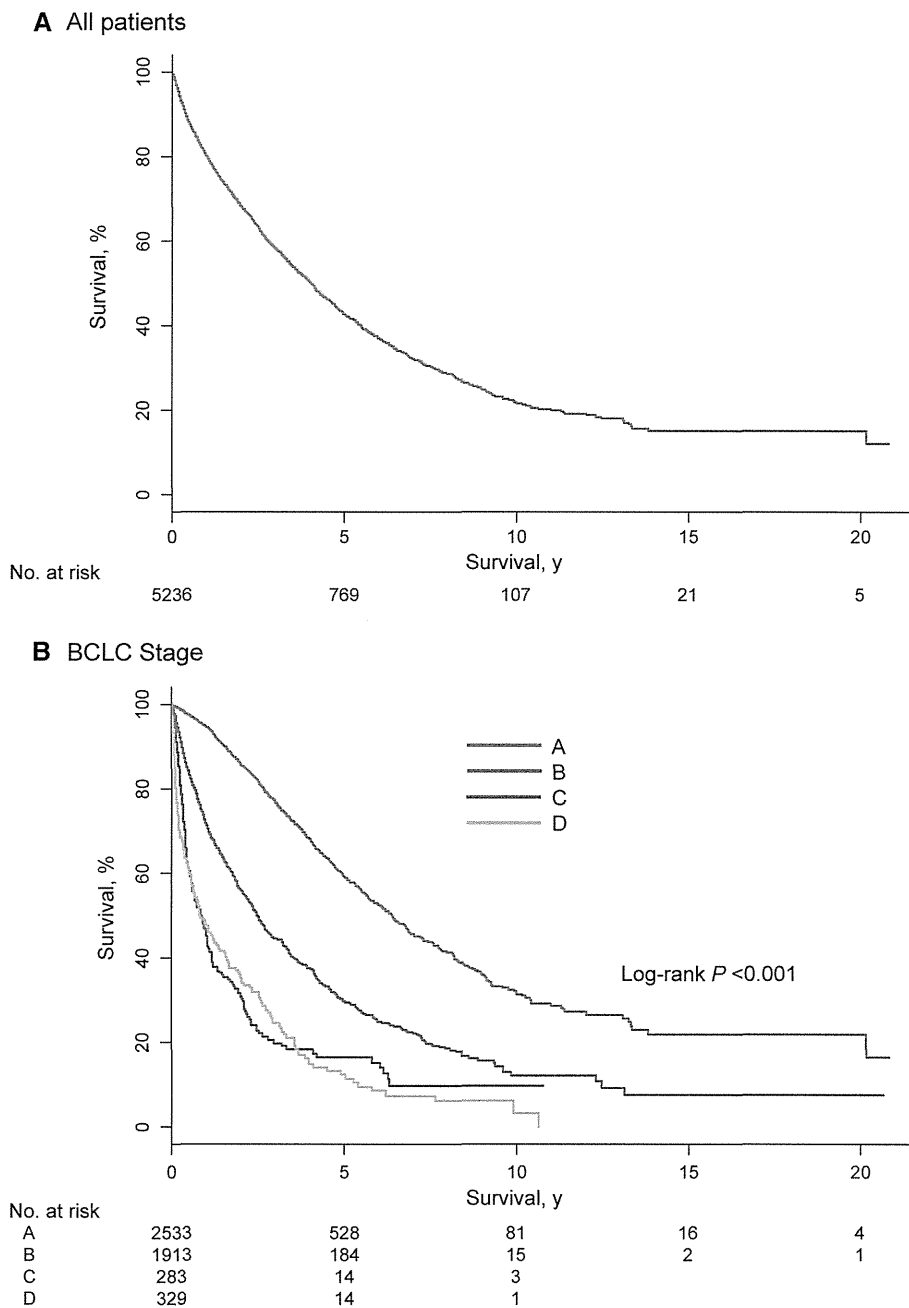
Table 2 Distribution of treatments according to BCLC stage

	A	B	C	D
Number of patients	2533	1913	283	329
Hepatic resection [n (%)]	616 (24.3)	398 (20.8)	30 (10.6)	3 (0.9)
Ablation [n (%)]	887 (35.0)	81 (4.2)	4 (1.4)	52 (15.8)
TACE + ablation [n (%)]	335 (13.2)	116 (6.1)	3 (1.1)	4 (1.2)
TACE [n (%)]	517 (17.1)	840 (43.9)	78 (27.6)	83 (25.2)
Transarterial chemotherapy [n (%)]	83 (3.2)	278 (14.5)	87 (30.7)	27 (8.2)
Systemic therapy [n (%)]	5 (0.2)	50 (2.6)	25 (8.8)	7 (2.1)
Radiation therapy [n (%)]	5 (0.2)	4 (0.2)	3 (1.1)	5 (1.5)
Liver transplantation [n (%)]	11 (0.4)	6 (0.3)	0(0.0)	0 (0.0)
Others [n (%)]	12 (0.5)	5 (0.3)	2 (0.7)	4 (1.2)
Supportive therapy [n (%)]	64 (2.5)	135 (7.1)	51 (18.0)	144 (43.8)

BCLC stage could not be determined in 268 patients
TACE transarterial chemoembolization

Fig. 3 Overall survival.

A Overall survival of the entire patient cohort. Overall survival rates at 1, 3, 5, 7, 10, 15, and 20 years were 80.1, 58.2, 42.6, 32.2, 21.5, 15.2, and 15.2 %, respectively. **B** Overall survival according to BCLC stage. Survival rates at 1, 3, 5, 7, 10, 15, and 20 years were 94.5, 76.4, 58.7, 44.7, 30.7, 21.9, and 21.9 % in stage A, 71.1, 44.1, 29.1, 22.2, 13.0, 9.0, and 9.0 % in stage B, 44.6, 18.8, 15.5, 9.3, and 9.3 % in Stage C, and 48.0, 24.4, 12.3, 7.3, 3.1 %, respectively, in Stage D



and 15.2 %, respectively (Fig. 3a). When stratified by BCLC stage, the median (95 % CI) survival times were 6.39 (5.96–6.85), 2.48 (2.34–2.68), 0.83 (0.61–1.03), and 0.80 (0.64–1.23) years in BCLC stages A, B, C, and D, respectively. There was a significant difference in survival among the stages (Fig. 3b, $p < 0.001$).

Univariate Cox regression analysis revealed that the following factors were significantly related to poor survival: old age ($p < 0.001$), male gender ($p = 0.003$), alcohol consumption ≥ 80 g/day ($p < 0.001$), BMI ($p = 0.001$), Child-Pugh score ($p < 0.001$), maximal tumor size ($p < 0.001$), number of nodules ($p < 0.001$), the

presence of vascular invasion ($p < 0.001$), the presence of extrahepatic metastasis ($p < 0.001$), AFP ($p < 0.001$), DCP ($p < 0.001$), and AFP-L3 ($p < 0.001$). The presence of diabetes was indicated as a better prognosis factor, though with marginal significance (hazard ratio, 0.93; 95 % CI, 0.86–1.01; $p = 0.08$). BMI showed a V-shaped hazard distribution: those with BMIs of 22.1–25 kg/m² had the best outcomes, whereas those with higher and lower BMI showed worse prognoses. We plotted relative hazard against BMI using cubic splines. The V-shape hazard distribution was also observed in the plot (Supplementary Fig. 2).

We performed a multivariate analysis using the variables above, except that AFP-L3 was excluded because of missing values. The results showed that age, BMI, alcohol consumption, Child-Pugh score, tumor size, number of tumor nodules, extrahepatic metastasis, AFP, and DCP were significant factors related to poor prognosis (Fig. 4). The presence of diabetes again showed no statistical significance.

Discussion

In the present study, a rapidly increasing proportion of HCC patients with non-viral etiologies was found. A similar trend was reported in a national survey by the Liver Cancer Study Group of Japan [18]. As the number of newly diagnosed HCC cases in Japan was almost at a plateau throughout the study period [19], not only the proportion,

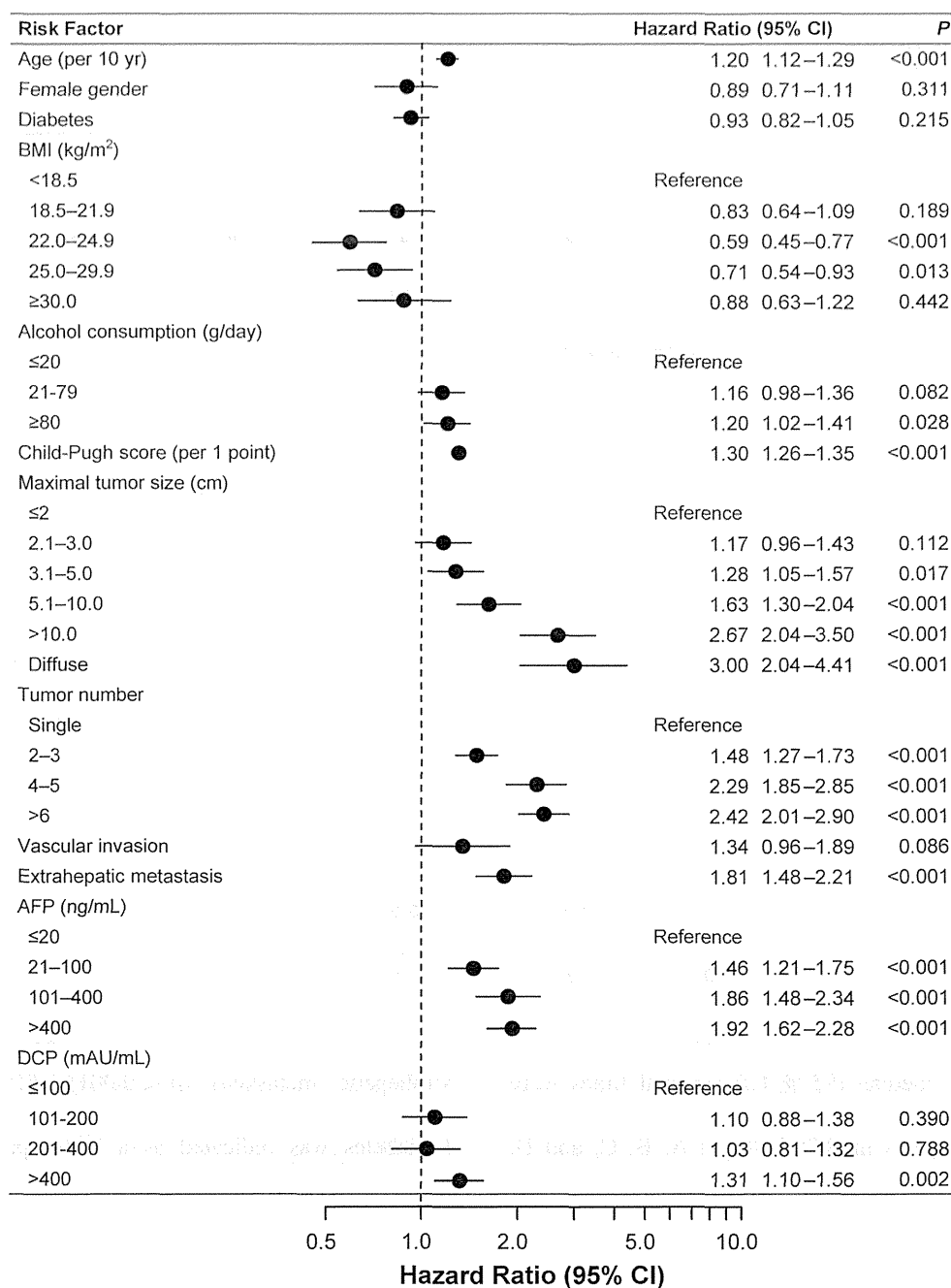


Fig. 4 Multivariate Cox proportional hazard regression analysis of survival. AFP alpha-fetoprotein, AFP-L3 lens culinaris agglutinin-reactive fraction of AFP, DCP des-gamma-carboxy prothrombin AFP alpha-fetoprotein, AFP-L3 lens culinaris agglutinin-reactive fraction

of AFP, ALT alanine aminotransferase, Anti-HBcAb anti-hepatitis B core antibody, DCP des-gamma-carboxy prothrombin, IQR interquartile range

but also the number, of patients with non-viral etiologies was increasing. As a risk factor of HCC, alcohol consumption has not increased over the last two decades in Japan according to statistics from the Ministry Labour and Welfare in Japan [20]. In contrast, the size of the obese population is increasing rapidly due to changes in the diet in Japan. The proportion of patients with diabetes has also increased in the past three decades [21]. It seems reasonable that the rapidly increasing number of HCC patients with non-viral etiologies was largely due to the rapidly increasing obese population.

Among non-viral chronic liver diseases, the natural history of AIH, PBC, and alcoholic liver disease are well known compared with that of NAFLD. In these three, HCC ordinarily arises through cirrhosis after long-lasting chronic inflammation in the liver [22–24]. Indeed, liver cirrhosis was a complication in more than 80 % of those patients. In contrast, the proportion of cirrhosis was smaller and platelet counts were higher in NAFLD patients than those with AIH, PBC, and alcoholic liver disease. It has been reported that a significant proportion of patients (41.7 %) with both NAFLD and HCC are not complicated with cirrhosis [25]. That a significant proportion of patients with NAFLD or unclassified etiology were not complicated with cirrhosis suggests that to characterize a high-risk population within them would be difficult.

In this study, almost half of the patients were complicated with diabetes mellitus. According to a systematic review investigating the relationship between diabetes and HCC, the presence of diabetes is an approximately 2.5-fold risk of HCC [26]. Judging from the wide variation in the proportion of patients with diabetes among the etiologies, it seems that diabetes correlates more strongly with hepatocarcinogenesis in some chronic liver diseases, such as NAFLD, than others.

In this study, we defined NAFLD as a history of fatty liver and alcohol consumption of no more than 20 g/day. As shown in Table 1, fatty liver was not diagnosed by ultrasonography at the diagnosis of HCC in approximately 30 % of patients with NAFLD-related HCC. Those patients would be categorized as unclassified when a history of fatty liver was not confirmed. That is, a significant proportion of those categorized as unclassified could be burn-out non-alcoholic steatohepatitis (NASH). Similarly, alcohol-related HCC could be included in unclassified patients because approximately 40 % of the patients in the category were moderate drinkers. In the first place, it might be unreasonable to categorize those patients clearly, because moderate alcohol intake, obesity, and fatty liver are mutually correlated and may have a synergistic effect on hepatocarcinogenesis.

Occult infection with HBV represented by the presence of antibody to hepatitis B core antigen (anti-HBc) has been

considered as a risk factor of non-B, non-C HCC defined as negative for both HBsAg and anti-HCV antibody [27, 28]. Indeed the prevalence of anti-HBc antibody was higher in this study compared to a previous report in blood donors [29]. It is also to be noted that those with anti-HBc antibody may include chronic HBV carriers with HBsAg loss before the diagnosis of HCC, who had significant risk for HCC [30].

Patients were diagnosed at less-advanced stages than we expected. This is partly because all participating hospitals were tertiary care centers. Those with terminal stages diagnosed in primary or secondary hospitals were unlikely to be referred to the participating hospitals. In addition, 41 % of patients were followed by imaging modalities before the diagnosis of HCC. As a result, a large majority of patients underwent radical therapies, such as hepatic resection, ablation, or TACE, as the initial treatment.

Prognostic factors for HCC have been investigated fully in previous studies [31]. However, to our knowledge, this is the first report of the detailed relationship between BMI and survival in HCC patients. Indeed, BMI showed a V-shaped hazard function for death. It is well known that the relationship between BMI and all-cause mortality is V-shaped, with a BMI around 22 kg/m² showing the best prognosis. However in this study, the lowest relative hazard was observed at a slightly overweight BMI. We had expected that the best BMI would be around 22 kg/m², because obesity is thought to affect hepatocarcinogenesis in this cohort and may affect recurrence after treatment. This would be because the relatively underweight patients included those with more advanced disease. However, the trend remained after adjustment for other significant factors, including those related to the tumor. Overweight patients may have some advantage versus underweight patients that we did not investigate.

The presence of diabetes did not affect survival in this study. One meta-analysis reported that the presence of diabetes increased the risk of all-cause mortality in HCC patients by 1.38-fold (95 % CI, 1.13–1.68) [32]. It is quite reasonable that those with diabetes had additional risk for death from cardiovascular, cerebrovascular, infectious or renal diseases. Some kind of biases might exist behind the fact that the presence of diabetes did not worsen the patients' survival, which needs further investigation.

Most of the major limitations of this study relate to its retrospective design.

(1) Because the major data source was a database maintained by each participating hospital, some data were missing. Patients who were not registered in the database could not be entered into this study. However, the proportion of patients with missing data on important items, such as alcohol consumption, was less than 5 %; this would not affect the overall results. (2) As the amount of daily